Tellus (1991), *43A*, 295–305

The dynamics of the zonal index in a simple model of the atmosphere

By WALTER A. ROBINSON, *University of Illinois at Urbana-Champaign, 105 South Gregory Avenue, Urbana, Illinois 61820, USA*

(Manuscript received 18 July 1990; in final form 25 March 1991)

ABSTRACT

A simple nonlinear global model with zonally symmetric forcing displays strong variability in its zonally averaged circulation on time-scales from weeks to months. These variations resemble the behavior of the zonal index in observations, especially in the Southern Hemisphere. In the model, as the zonal index varies, synoptic eddies and their associated fluxes follow the strongest westerlies poleward and equatorward. Synoptic fluxes of momentum sustain the index against dissipation, and are responsible for its persistence. While the momentum fluxes by low-frequency eddies are not well correlated with the index, they are significant in determining its tendency.

1. Introduction

Among the rich variety of low-frequency motions in the atmosphere are fluctuations in the extra-tropical, zonally averaged circulation. It has long been recognized that the zonal index, typically defined as the average strength of the zonal winds between 35 and 55°, gives a concise description of such fluctuations (Willett, 1948). 40 years ago, the "index cycle" was introduced to describe the evolution of the zonal index (Namias, 1950). The "cycle" suggests a recurring sequence of events, though possibly with varying strength and duration. According to Namias, the index decreases from an initially high value when blocking waves and strong occluded cyclones develop. Cold air escapes from the polar vortex, and the strongest westerlies reform equatorward of the eddies. This is the low index phase. The index recovers when the eddies weaken and radiative cooling rejuvenates the polar vortex.

More recently, cognizance of the importance of zonal asymmetries in the time-averaged circulation (Blackmon et al., 1977) has cast doubt on the theory of the index cycle, in that it requires simultaneous outbreaks of eddy activity at widely separated longitudes. Wallace and Hsu (1985) failed to find, at least in the Northern Hemisphere, the negative correlation between eddy activity and zonal index required by Namias' theory. From this, they suggested that observed fluctuations in zonally symmetric quantities are perhaps only the statistical residue of dynamically unrelated events at different longitudes.

In the face of these arguments, the index cycle has almost vanished from modern meteorology. Interest in zonally symmetric variability, however, has survived, especially for the Southern Hemisphere. In a single year of data collected by constant density balloons Webster and Keller (1975) found hemispheric fluctuations in the zonally averaged circulation with periods of 18 to 23 days. Trenberth (1979) found strong interannual variability in the zonally averaged zonal winds at 500 mb in spring and summer in six years of Southern Hemisphere synoptic analyses from the Australian Bureau of Meteorology. Rogers and van Loon (1982) computed Empirical Orthogonal Functions (EOF's) from the same data. The leading patterns in sea-level pressure and 500 mb geopotential for winter and for summer are nearly zonally symmetric and are all similar. Heights or pressures poleward of 50°S rise and fall in opposition to those at lower latitudes.

These studies showed the importance of zonally symmetric low-frequency variability in the Southern Hemisphere. Some recent work has focused on the zonal index. Kidson (1986)

calculated a zonal index (ZI), defined as the difference between the zonally averaged zonal winds in bands centered on 67.5 and 48.75° S, for the austral winter of 1979, the year of the Global Weather Experiment. Composites of the 500 mb zonal winds for high values of ZI reveal a single jet at around 50° S nearly circumscribing Antarctica. For low ZI, the subpolar jet is weaker, and there is a separate jet near 30° S over half the hemisphere. During this winter ZI oscillated irregularly with a period of about 27 days.

Kidson (1988) later examined zonally averaged zonal winds from 15 years of Australian Southern Hemispheric analyses. He found the strongest variability at periods greater than 50 days. These fluctuations are strongly correlated across latitudes. The leading EOF has a minimum at 37.5° S and a maximum at 57.5° S, crossing zero at about 50°; i.e., the zonal winds north of 50° vary together and in opposition to the winds farther south. When the data were filtered, similar results were obtained separately for different timescales.

While not as convincing as for the Southern Hemisphere, there is evidence for significant zonally symmetric variability in the Northern Hemisphere. Lorenz (1951) found strong negative correlations between geostrophic zonal wind anomalies at 20–30° N and at 50–60° N, in pentads of zonally averaged sea-level pressures from the 1930's. Kidson (1985) explored variations in the Northern Hemisphere zonal index during the winter 1978–79. While his results are similar to those for the Southern Hemisphere, in the Northern Hemisphere variability is dominated by the North Atlantic jet. Finally, Branstator (1990) found that the second leading EOF for the 300 mb streamfunction in a 6000 day run of a general circulation model, NCAR CCMOB, is strongly zonal, with maxima over the Atlantic and Pacific jets and minima to the north and south. This pattern represents simultaneous meridional excursions by the two jets in the model.

The dynamics of these zonal variations is unclear. Webster and Keller suggested that momentum fluxes by ultra-long planetary waves were responsible, while Kidson (1986) thought that blocking might be important. Karoly (1990) showed that variations in transient (defined as deviations from the monthly mean) eddy fluxes parallel those in the zonal index, such that the fluxes reinforce the monthly anomalies in the zonal flow. Unfortunately, his data were not sufficiently reliable to permit the further decomposition of the transients into different timescales.

The present study was motivated by the author's analysis of low-frequency variability in a simple, zonally homogeneous, model of the atmosphere (Robinson, 1990). At periods longer than a month the variability in this model is primarily zonally symmetric, while on shorter time-scales it is dominated by Rossby wave-trains. In the following, we investigate the appearance and dynamics of the zonally symmetric variability in this simple model, with the implication that the responsible mechanisms also may be relevant to the zonal index in the atmosphere. The emphasis is on how synoptic and low-frequency waves each contribute to the maintenance and variability of the zonal index.

2. The model

The present model, while independently coded, is nearly identical to that of Hendon and Hartmann (1985). The reader is referred to their paper for the model equations and the values of parameters. Briefly, this is a global, dry, two-level, spectral, primitive equation model in pressure coordinates. The present simulation is a "perpetual January." Newtonian relaxation mimicks radiative transfer, and linear drag on winds at the lower level, 750 mb, represents boundary layer dissipation. Subgridscale diffusion is included. The model is run at a rhomboidal 15 truncation.

The advantages of this model are its simplicity and computational speed. Because the pressure vertical velocity is assumed to vanish at 1000 mb, the model has only 5 prognostic variables at each horizontal location: vorticity and potential temperature at 750 and 250 mb, and the difference between the 250 and 750 mb divergence. At R15 truncation this corresponds to 2480 prognostic variables for the global model. With a timestep of one hour, the integration of a model day requires 0.7 seconds of computing time on the Cray XMP computer at the National Center for Supercomputing Applications. The simplicity of the model similarly aids in diagnostic calculations. The storage requirements for model output data are slight, and dynamical budgets may be computed quickly.

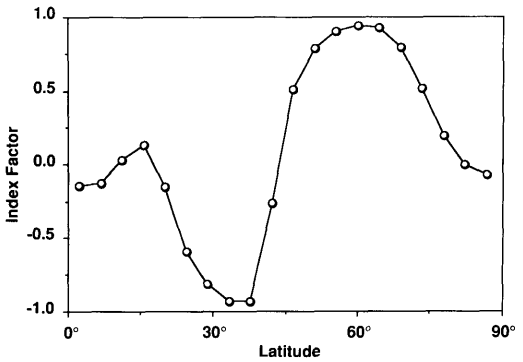

Fig. 1. Structure of the leading rotated EOF of the zonally averaged zonal angular momentum computed from 10-day low pass data. The projection of the 10-day low pass angular momentum onto this vector defines the zonal index.

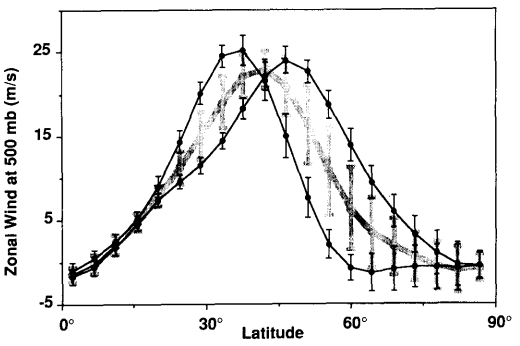

Fig. 2. Composites of the zonally averaged zonal wind at 500 mb for the highest and lowest 10% of values of the zonal index, sampled every 5th day. The heavy shaded curve is the model climatology. Error bars indicate one standard deviation.

The cost of this dynamical and computational simplicity is an overly simple representation of the atmosphere. In particular, the vertical structure is described with only two degrees of freedom. While this would not be sufficient for a detailed simulation of the climate, there is ample evidence that the two-level model adequately represents the principal modes of atmospheric variability (Hendon and Hartmann, 1985; Kushnir and Esbensen, 1986).

3. Behavior of the zonal index

For the present study, the *zonal index* is defined as the factor score of the leading EOF of the Northern Hemisphere zonally averaged angular momentum. The procedure for its calculation is as follows: Twice-daily model output from the final 1440 days of a 1500-day run is filtered with a 10-day low-pass filter (Blackmon, 1976), and the time means are removed. The filtered angular

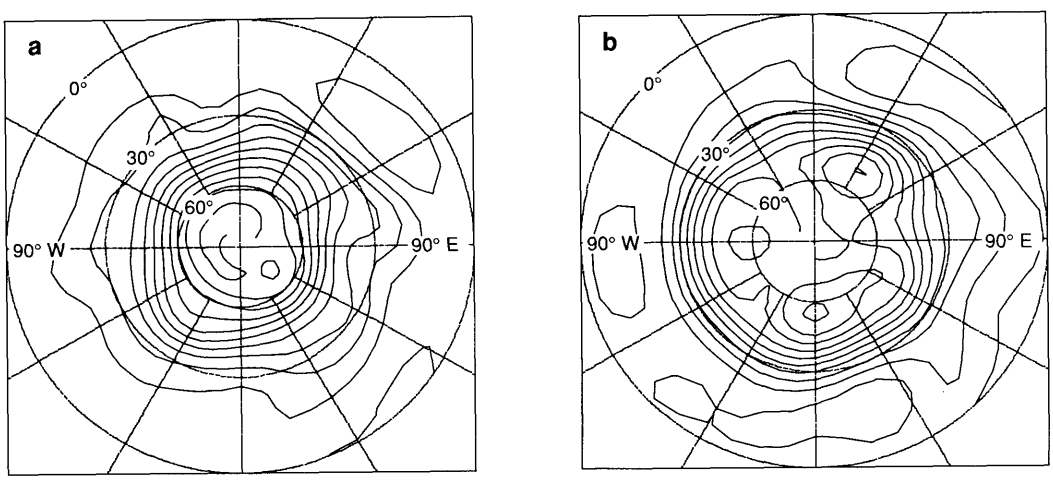

Fig. 3. Low-frequency (10-day low pass) 500 mb streamfunction. The contour interval is 10^7 m^2 s^{-1}. (a) Day 92; the zonal index is 11.7. (b) Day 607; the zonal index is -13.0.

momentum, averaged over pressure and longitude, is sampled at the 20 Gaussian latitudes in the Northern Hemisphere every 5 days. These data are analyzed using the factor analysis routines of the Stat View II™ software package for the MacIntosh personal computer. The four leading eigenvectors are subjected to an orthogonal rotation using the VARIMAX procedure, and the first leading rotated EOF is selected as the "zonal index," denoted by Z. (In this case the leading rotated EOF is indistinguishable from the leading unrotated function.)

The meridional structure of the leading factor is shown in Fig. 1. This pattern explains 41% of the variance of the filtered Northern Hemisphere angular momentum. It captures the most striking feature of the correlation matrix from which it is computed, the strong negative correlations between zonally averaged zonal winds at subtropical and middle latitudes. For example, the correlation between the filtered zonal winds at 29°N and 51°N is −0.906. The present index is also consistent with the traditional zonal index: the correlation between Z and the mean zonal wind between 38° and 55.5°N, both filtered and sampled daily, is 0.79.

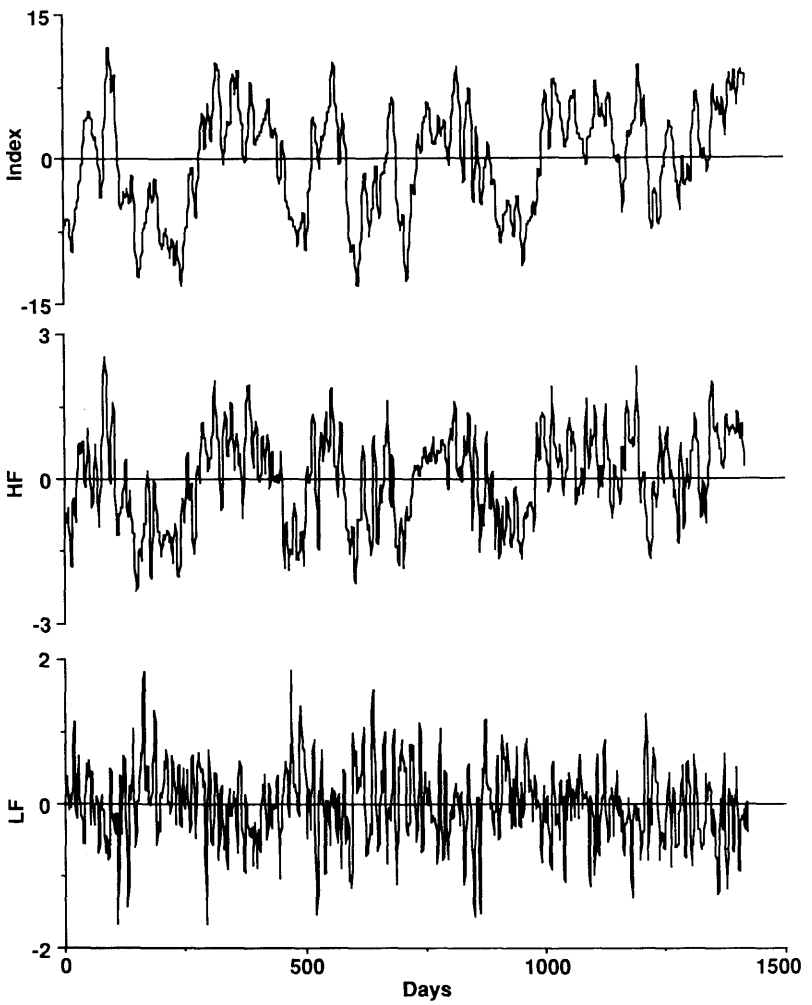

Fig. 4. Daily values of the zonal index, and its forcing by high- and low-frequency eddies (see Section 4).

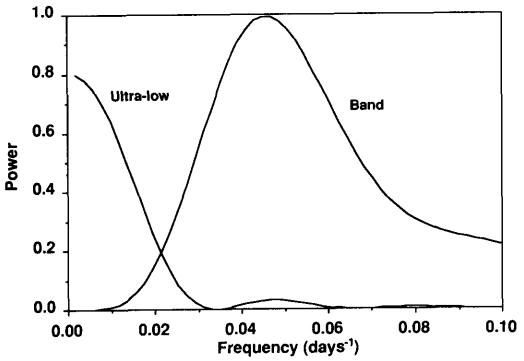

Fig. 5. Responses of the ultra-low pass and band-pass filters in terms of power.

Composites of the zonally averaged zonal winds for the highest and lowest 10% of values of the zonal index (Fig. 2) show the structure of the zonal flow in low and high index states. When the index is high, the jet lies poleward of its climatological latitude, and relatively strong westerlies extend into subpolar latitudes. In low-index states, the jet is displaced equatorward, and the zonal flow poleward of 60° is very weak. Fig. 3 shows the 10-day low pass filtered 500 mb streamfunction for a day with a very high index (Fig. 3a) and a day with a very low index (Fig. 3b). The high index flow has a tight polar vortex with a single central low, while in the low index flow the vortex has expanded nearly to 30° and comprises 3 separate lows.

Fig. 4 shows the behavior of the zonal index over time. There is variability on a wide range of time-scales, and it appears that the longest periods contain the most power. This is confirmed by spectral analysis of daily values of the zonal index calculated using unfiltered data from an extended run of the model (6000 days). The power spectrum of this time series is flat for frequencies less than 0.01 days^{-1}, but then decreases by nearly two orders of magnitude between 0.01 and 0.1 days^{-1}. The logarithmic spectrum (e.g., Zangvil, 1981), the power spectrum multiplied by the frequency, has a strong peak at frequencies slightly greater than 0.01 days^{-1}.

The longest time-scales can be isolated by smoothing the time-series using a 31-day moving average. Filtering the twice-daily model output with a 10-day low pass filter, sampling every other value, then applying a 31-day running mean defines an "ultra-low" pass filter, the response of which is shown in Fig. 5. Power is reduced by one half at a period of about 70 days. The difference between the "ultra-low" pass filtered and the 10-day low pass filtered series defines a band-pass filter, also shown. Fig. 6 shows 5800 days of the ultra-low frequency index sampled every 10th day. On these long time-scales the index makes occassional excursions to large negative values.

The frequency distributions of the index are

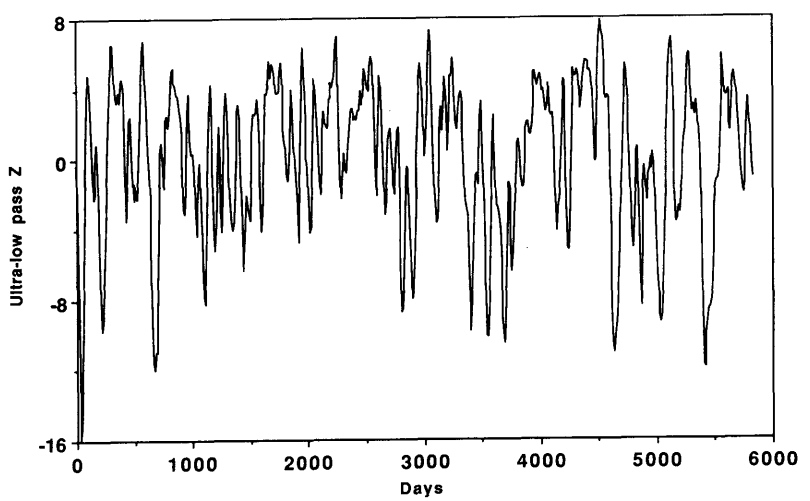

Fig. 6. Time series of the ultra-low pass filtered zonal index, sampled every 10th day.

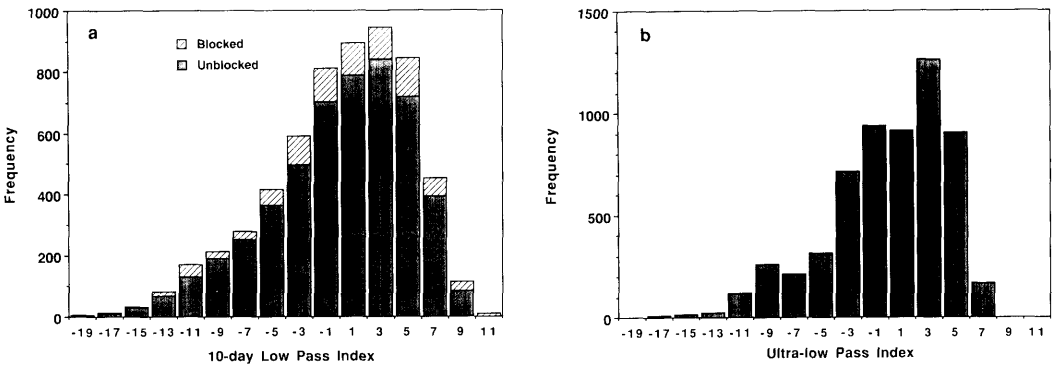

Fig. 7. Histograms of daily values of the zonal index. (a) Values computed from 10-day low-pass data, distinguishing blocked and unblocked days (see Section 5). (b) Values computed from ultra-low pass data.

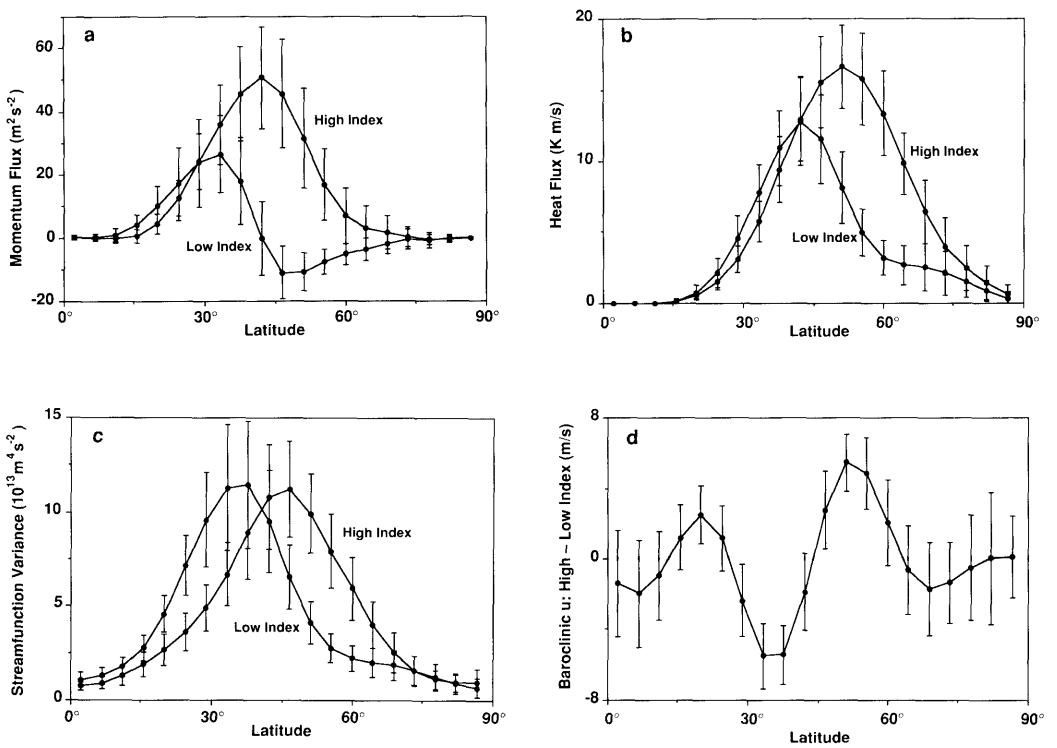

Fig. 8. Composites for the highest and lowest 10% of values of the zonal index, computed from 10-day low pass filtered data sampled every fifth day. The vertical bars show the standard deviations within each composite. (a) Meridional flux of zonal momentum by synoptic (10-day high pass) eddies at 250 mb. (b) Meridional flux of heat at 500 mb by synoptic eddies. (c) Variance of the synoptic streamfunction at 250 mb. (d) Difference of the baroclinic component of the zonal wind, u(250 mb)–u(750 mb), between the high and low index composites.

strongly skewed, both on the 10-day low-pass (Fig. 7a) and ultra-low-pass (Fig. 7b) time-scales. The histograms are calculated from the 6000 day run of the model. The complex structure at negative values of Z is a consequence of the sporadic excursions of Z to large negative values.

The effects of the zonal index on the general circulation of the model can be seen in composites of high and low values. Fig. 8 shows such composites for three properties of the synoptic (10-day high pass) eddies: the meridional flux of zonal momentum at 250 mb, the northward flux of heat at 500 mb, and the variance of the eddy streamfunction at 250 mb. These quantities are computed from the 10-day high pass filtered fields, forming the appropriate flux, applying the 10-day low-pass filter, and zonally averaging. The composites are formed for the highest and lowest 10% of values of the zonal index, sampled every five days, so that each curve is an average over 28 days. The vertical bars indicate the standard deviations of these 28 member samples.

Fig. 8 suggests a self-consistent physical picture of the high and low index states. High and low index states clearly differ in the behavior of synoptic eddies. The momentum fluxes by the synoptic eddies act to support the index, i.e., the strongest convergence of westerly momentum is about 15° further north in the high index than in the low index composite. The eddy variance and the northward heat flux show that baroclinic activity is strongest near the jet maximum in both cases. A surprising result is that the overall baroclinic activity, as indicated by the northward flux of heat (Fig. 8b), is significantly stronger in the high index composite (weighting by the cosine of latitude does not eliminate the difference in the areas under the two curves). Because this difference does not appear in the eddy variance, the synoptic eddies in high index flows must be more efficient in transporting heat poleward than when the index is low.

The distributions of baroclinic activity in the high and low index composites are consistent with differences in the baroclinicity of the zonal flow. Fig. 8d shows the difference in the baroclinic component of the zonally averaged zonal wind, u (250 mb)–u (750 mb), between the high- and low-index composites. High-index flows are more baroclinic between 30 and 40° and less so around 50° than low-index flows. In comparison with Fig. 2, it can be seen that the structure of the zonal index is not barotropic, but has a strong baroclinic component with similar meridional structure to the vertically averaged index.

The results of these composites are confirmed by correlational analyses. The leading EOF's of the synoptic heat and momentum fluxes (not shown) closely resemble the differences between the high and low index composites shown in Fig. 8. Also, the correlations of the factor scores for the heat and momentum fluxes with the zonal index are greater than 0.65.

4. Dynamics of the zonal index

Having described the features of the circulation associated with high and low zonal index, we analyze how the index is maintained and modified. For the two-level model the equation for the zonal wind averaged over pressure and longitude is,

$$\bar{u}_t = -\frac{\overline{[uv\cos^2(\phi)]}_\phi}{a\cos^2(\phi)} - \bar{D}, \tag{1}$$

where the overbar denotes an average over longitude and pressure, and $\bar{D}$ denotes drag. There is no coriolis term, because in this two-level model, $\bar{v} = 0$. The evolution of the angular momentum in a zonal annulus at latitude ϕ, $\Lambda(\phi) = a\bar{u}\cos^2(\phi)$, is obtained by multiplying eq. (1) by $a\cos^2(\phi)$, where a is the radius of the earth. The tendency of the zonal index is obtained by projecting the equation for Λ_t onto the meridional structure of the EOF (Fig. 1), i.e.,

$$Z_t = \int_0^{\pi/2} \Lambda_t F(\phi)\, d\phi, \tag{2}$$

where Z is the zonal index and F is the EOF. Substituting from eq. (1) and integrating by parts gives,

$$Z_t = -F(0)\,\overline{uv}|_0 - \int_0^{\pi/2} \overline{uv} F_\phi \cos^2(\phi)\, d\phi - \text{drag}. \tag{3}$$

In practice, the first term on the right-hand side is small.

The momentum flux in eq. (3) can be separated into contributions from the synoptic (10-day high pass) and low-frequency (10-day low pass) eddies.

Table 1. *Variances of high- and low-frequency eddy contributions to the evolution of the zonal index, and their correlations with the index and its tendency*

Quantity	Total HF	Total LF	Ultra-low HF	Ultra-low LF	Band-pass HF	Band-pass LF
variance	0.86	0.26	0.47	0.05	0.32	0.22
correlation with Z	0.79	−0.34	0.93	−0.71	0.49	−0.12
correlation with Z_t	0.41	0.37	0.27	0.03	0.55	0.49

Recalling that Z is calculated from 10-day low pass data, these contributions also must be filtered. There are also contributions to Z_t from the interactions of the high and low frequency eddies that need not vanish. These, with the effects of the diffusion in the model, comprise a residual. The tendency of Z can then be written,

$$Z_t = \mathrm{HF} + \mathrm{LF} - \mathrm{drag} + \mathrm{residual}, \qquad (4)$$

where HF and LF are the contributions from the 10-day high pass and 10-day low pass eddies.

Time series of HF and LF are shown in Fig. 4. The forcing of the index by synoptic eddies, HF, is strongly correlated with Z, especially on longer time-scales and leads it slightly. In contrast, the forcing by low-frequency eddies, LF, displays more variability on shorter time-scales, and is much less well correlated with Z.

Table 1 shows the variances of HF and LF, and the correlations of HF and LF with Z and Z_t. At periods greater than 70 days the flux of momentum by synoptic eddies dominates that of the low-frequency eddies. The forcing by the synoptic eddies correlates extremely well with the zonal index, implying that the synoptic eddies tend to sustain the index against dissipation, consistent with the composites in Section 3. The low-frequency eddies tend to erode the index, but this term is weak at the ultra-low frequencies. In the 10–70 day band the synoptic forcing is still correlated with the index, but not so strongly as at longer periods.

These relationships are displayed graphically in Fig. 9. Here, each term in eq. (4) is represented by a vector, the components of which are the correlations of that term with Z and with Z_t, both

Table 2. *Variances of Z_t, residual, and the residual when LF is excluded*

Frequencies	Variance of Z_t	Residual	Residual with LF excluded
all	0.44	0.09	0.30
ultra-low	0.04	0.01	0.06
band-pass	0.41	0.08	0.26

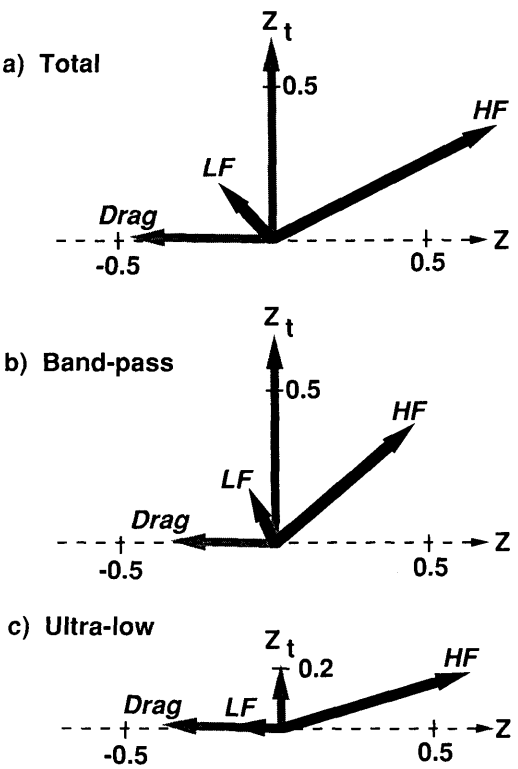

Fig. 9. Vector diagrams indicating the contributions to the index and its tendency from high-frequency eddies (HF), low-frequency eddies (LF) and drag. The vertical and horizontal components of each vector represents the correlation of each quantity with Z_t and Z. Lengths are scaled by the square root of the variance of each quantity. (a) 10-day low pass quantities. (b) Band-pass quantities. (c) Ultra-low pass quantities.

weighted by the square root of the variance of that term. Thus these diagrams show the dynamical balances that both maintain the index and cause it to change over time. On all time-scales it is seen that the synoptic eddies sustain the index against dissipation and are the principal cause of its tendency. The low-frequency eddies act with Drag in opposition to HF; on band-pass time-scales they also make a significant contribution to Z_t.

Despite the relatively small variance of LF it is important in the determination of the tendency. As is shown by Table 2, when LF is included the variance of the residual in eq. (4), is 25% or less of the variance of Z_t. When LF is left out, however, the variance of the residual is of the same order as that of Z_t. In other words, if the future state of the zonal index is to be forecast, the effects of synoptic eddies, low-frequency waves, and dissipation must all be included.

5. The zonal index and blocking

Some earlier studies have associated variations in the zonal index with the occurrence of blocking (Namias, 1950; Kidson, 1986). In the present study, blocks were determined objectively using the criteria of Lejenäs and Økland (1983) as adopted by Tibaldi and Molteni (1990). This involves searching the unfiltered 500 mb streamfunction fields for days on which the rotational flow is easterly in middle northern latitudes. Blocks are distinguished from days on which the westerly jet and polar easterlies are displaced equatorward by requiring the process of westerly flow poleward of the block. In the 6000-day run, blocks are present on about 13.5% of the model days. This is comparable to the frequency found by Tibaldi and Molteni, though in this model, the frequency of blocking is zonally uniform.

The mean value of the zonal index on the 789 blocked days, 0.03, is indistinguishable from zero. This suggests that blocking is not a critical component of the variations in the zonal index. Blocks occur in flows with very high and very low values of the zonal index. Fig. 10a shows a block near 90° E on day 560, when the zonal index is 8.8, while Fig. 10b shows a block at a similar longitude on day 595 when the index is −9.5.

The strongest statement that can be made regarding the connection between blocking and the zonal index is that the probability of blocking increases when the index is at a positive or negative extreme. Blocks occur on 15.7% of the days for which the index is in its lowest 10 percentiles ($Z \leqslant -7.5$), and on 16.6% of the days when the index is in its highest ten percentiles ($Z > 6.0$). In flows with a very high index, the jet is displayed well to the north, and blocks can easily form equatorward of the jet. When the index is very low, blocks can form on its poleward flank.

In general, however, blocks and variations in the index are phenomenon that in the model occur on

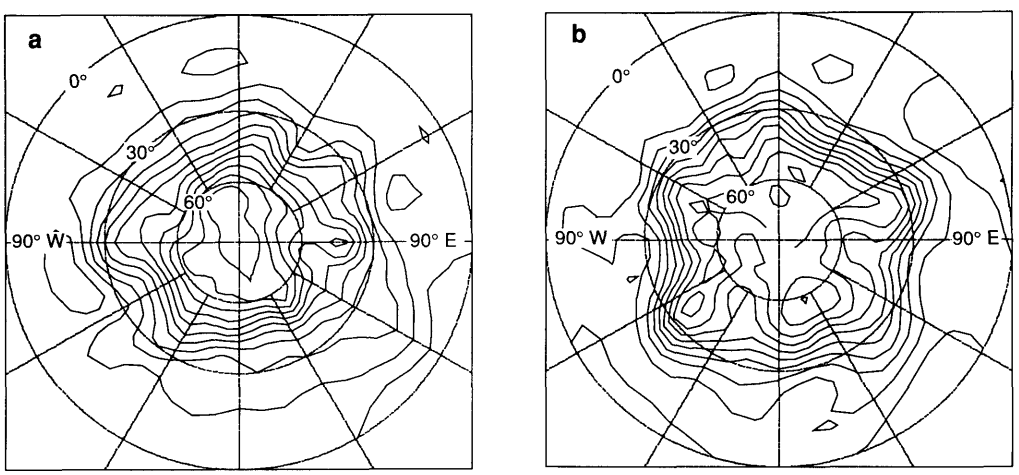

Fig. 10. Unfiltered 500 mb streamfunction during two different blocks near 90° E. The contour interval is 10^7 m^2 s^{-1}. (a) Day 560; the zonal index is 8.8. (b) Day 595; the zonal index is −9.5.

very different time-scales. Blocks persist for a few days while the dominant fluctuations in the zonal index are on time-scales of a month and longer.

6. Summary

A dry, zonally homogeneous, two level spectral model displays variations in the zonally averaged circulation that resemble fluctuations of the zonal index that have been observed in the atmosphere, especially the Southern Hemisphere. In the model the zonal index is strongly persistent on time-scales of a month and longer, and, through variations in baroclinicity, it organizes the average behavior of synoptic eddies. These properties are associated in that the momentum fluxes of the synoptic eddies maintain high or low index flows against dissipation. High values of the zonal index are somewhat more persistent than low values (Figs. 4, 6, and 7), probably because there is more baroclinic activity when the index is high (Fig. 8b).

To a rough approximation, the index at any time represents a balance between dissipation and forcing by the momentum fluxes of the synoptic eddies, and this is especially true on longer time-scales. The tendency of the index derives from the relatively small difference between these terms together with the forcing by the low-frequency waves.

In contrast to some theories of the index cycle, e.g., Namias (1950), it appears that blocking is not important in the variations of the zonal index in this model, though blocking is somewhat more frequent for extreme values of the index. There is also no evidence of a split or double jet in the model, as was found in the Southern Hemisphere by Kidson (1986) and Yoden et al. (1987). Interestingly, the transitions between single and double jet regimes found by the latter authors correlate well with the leading EOF of the zonal wind, and this EOF has a meridional structure strikingly similar to the pattern that defines the zonal index in the present work (Fig. 1). Perhaps the appearance of the double jet is not crucial to the dynamics of the variability, but comes about from superimposing such variability on a climatological circulation that, because of conditions at the lower boundary, tends to support both subtropical and subpolar jets.

Future work will explore the predictability of the zonal index in longer model simulations, the robustness of its persistence in a model with an annual cycle, and its behavior in a model with orographically forced stationary waves. The predictability is of particular interest, because of the paradoxical role played by synoptic eddies. In this model, as in the atmosphere, they are the principal source of the overall loss of predictability, but through their transport of momentum they are responsible for the persistence of the zonal index beyond the dissipative time-scale of 10 days. In this way, they create the possibility of enhanced predictability for the zonally averaged circulation in the model. Perhaps synoptic waves also play such a dual role in the atmosphere.

7. Acknowledgments

This research was supported by the Climate Dynamics Program of the United States National Science Foundation, grant ATM 8815184. Computations were performed on the Cray XMP and YMP computers at the National Center for Supercomputing Applications.

REFERENCES

Blackmon, M. L. 1976. A climatological spectral study of the 500 mb geopotential height of the Northern Hemisphere. *J. Atmos. Sci. 33*, 1607–1623.

Blackmon, M. L., Wallace, J. M., Lau, N.-C. and Mullen, S. L. 1977. An observational study of the Northern Hemisphere wintertime circulation. *J. Atmos. Sci. 34*, 1040–1053.

Branstator, G. 1990. Low-frequency patterns induced by stationary waves. *J. Atmos. Sci. 47*, 629–648.

Hendon, H. H. and Hartmann, D. L. 1985. Variability in a nonlinear model of the atmosphere with zonally symmetric forcing. *J. Atmos. Sci. 42*, 2783–2797.

Karoly, D. J. 1990. The role of transient eddies in low-frequency zonal variations in the Southern Hemisphere circulation. *Tellus 42A*, 41–50.

Kidson, J. W. 1985. Index cycles in the Northern Hemisphere during the Global Weather Experiment. *Mon. Wea. Rev. 113*, 607–623.

Kidson, J. W. 1986. Index cycles in the Southern Hemisphere during the Global Weather experiment. *Mon. Wea. Rev. 114*, 1654–1663.

Kidson, J. W. 1988. Indices of the Southern Hemisphere zonal wind. *J. Climate 1*, 183–194.

Kushnir, Y. and Esbensen, S. K. 1986. Northern Hemisphere wintertime variability in a two-level general circulation model. Part I: statistical characteristics of short and long time-scale disturbances. *J. Atmos. Sci. 43*, 2968–2984.

Lejenäs, H. and Økland, H. 1983. Characteristics of Northern Hemisphere blocking as determined from a long time series of observational data. *Tellus 35A*, 350–362.

Lorenz, E. N. 1951. Seasonal and irregular variations of the Northern Hemisphere sea-level pressure profile. *J. Meteor. 8*, 52–59.

Namias, J. 1950. The index cycle and its role in the general circulation. *J. Meteor. 7*, 130–139.

Robinson, W. A. 1991. The dynamics of low-frequency variability in a simple model of the global atmosphere. *J. Atmos. Sci. 48*, 429–441.

Rogers, J. C. and van Loon, H. 1982. Spatial variability of sea level pressure and 500 mb height anomalies over the Southern Hemisphere. *Mon. Wea. Rev. 110*, 1375–1392.

Tibaldi, S. and Molteni, F. 1990. On the operational predictability of blocking. *Tellus 42A*, 343–365.

Trenberth, K. E. 1979. Interannual variability of the 500 mb zonal mean flow in the Southern Hemisphere. *Mon. Wea. Rev. 107*, 1515–1524.

Wallace, J. M. and Hsu, H.-H. 1985. Another look at the index cycle. *Tellus 37A*, 478–486.

Webster, P. J. and Keller, J. L. 1975. Atmospheric variations: vacillations and index cycles. *J. Atmos. Sci. 32*, 1283–1300.

Willet, H. C. 1948. Patterns of world weather changes. *Trans. Amer. Geophys. Union 29*, 803–809.

Yoden, S., Shiotani, M. and Hirota, I. 1987. Multiple planetary flow regimes in the Southern Hemisphere. *J. Meteor. Soc. Japan 65*, 571–585.

Zangvil, A. 1981. Some aspects of the interpretation of spectra in meteorology. *Boundary-Layer Meteorology 21*, 39–46.